Journal of Physics: Conference Series

PAPER • **OPEN ACCESS**

A carbon minibeam irradiation facility concept

To cite this article: M Mayerhofer *et al* 2023 *J. Phys.: Conf. Ser.* **2420** 012097

Journal of Physics: Conference Series **2420** (2023) 012097 doi:10.1088/1742-6596/2420/1/012097

A carbon minibeam irradiation facility concept

M Mayerhofer[1], V Bencini[2], M Sammer[1] and G Dollinger[1]

[1] Universität der Bundeswehr München, 85579 Neubiberg, Germany
[2] University of Oxford, OX1 2JD Oxford, United Kingdom

E-mail: michael.mayerhofer@unibw.de

Abstract. In minibeam therapy, the sparing of deep-seated normal tissue is limited by transverse beam spread caused by small-angle scattering. Contrary to proton minibeams, helium or carbon minibeams experience less deflection, which potentially reduces side effects. To verify this potential, an irradiation facility for preclinical and clinical studies is needed. This manuscript presents a concept for a carbon minibeam irradiation facility based on a LINAC design for conventional carbon therapy. A quadrupole triplet focuses the LINAC beam to submillimeter minibeams. A scanning and a dosimetry unit are provided to move the minibeam over the target and monitor the applied dose. The beamline was optimized by TRAVEL simulations. The interaction between beam and these components and the resulting beam parameters at the focal plane is evaluated by TOPAS simulations. A transverse beamwidth of $< 100\,\mu m$ (sigma) and a peak-to-valley (energy) dose ratio of > 1000 results for carbon energies of 100 MeV/u and 430 MeV/u (~ 3 cm and 30 cm range in water) whereby the average beam current is ~ 30 nA. Therefore, the presented irradiation facility exceeds the requirements for hadron minibeam therapy.

1. Introduction

Compared to proton or heavy ion radiotherapy, minibeam radiation therapy has the potential to further spare normal tissue [1, 2]. The dose required for tumor control is applied through minibeams with an inital transverse width in the submillimetre range. Pencil or planar minibeams are arranged in a grid or an array with a center-to-center distance (ctc) of a few millimeters [3, 4]. The resulting transverse dose distribution with dose minima between minibeam channels spares normal tissue compared to broad beams, reducing side effects. The lateral width of the beams increases with penetration depth due to small-angle scattering. With a suitable ctc, the individual minibeams superimpose in the tumor resulting in a homogeneous dose [5]. The potential of minibeam therapy has been confirmed by preclinical experiments for protons [1, 2, 6–9]. However, it has been shown that the normal tissue sparing decreases with increasing transverse beam width [8]. Therefore, especially the sparing of the deeper normal tissue is limited due to the spreading of the proton beam. In comparison, heavier hadrons such as helium or carbon are less affected by small-angle scattering, which offers the possibility to enhance normal tissue sparing [5, 10, 11]. To evaluate the potential of heavy ions for minibeam therapy in (pre)clinical studies, an irradiation facility needs to be established. Here, we focus on a carbon minibeam facility that could easily be adapted to a helium minibeam facility. Thereby the following requirements should be fulfilled: 1. a carbon ion range in water from 3 cm to 30 cm. 2. a beam current > 1 nA to allow single-session treatments. 3. a transverse beam width of 100 µm and a peak-to-valley dose ratio (PVDR) of > 540 which causes no normal tissue

reaction for proton minibeams [8] 4. a possibility for beam scanning up to $X = Y = \pm 15$ mm that would be sufficient for preclinical experiments as well as for first clincial trials. This manuscript shows a LINAC-based concept for a carbon (helium ion) minibeam irradiation facility that fulfils these requirements.

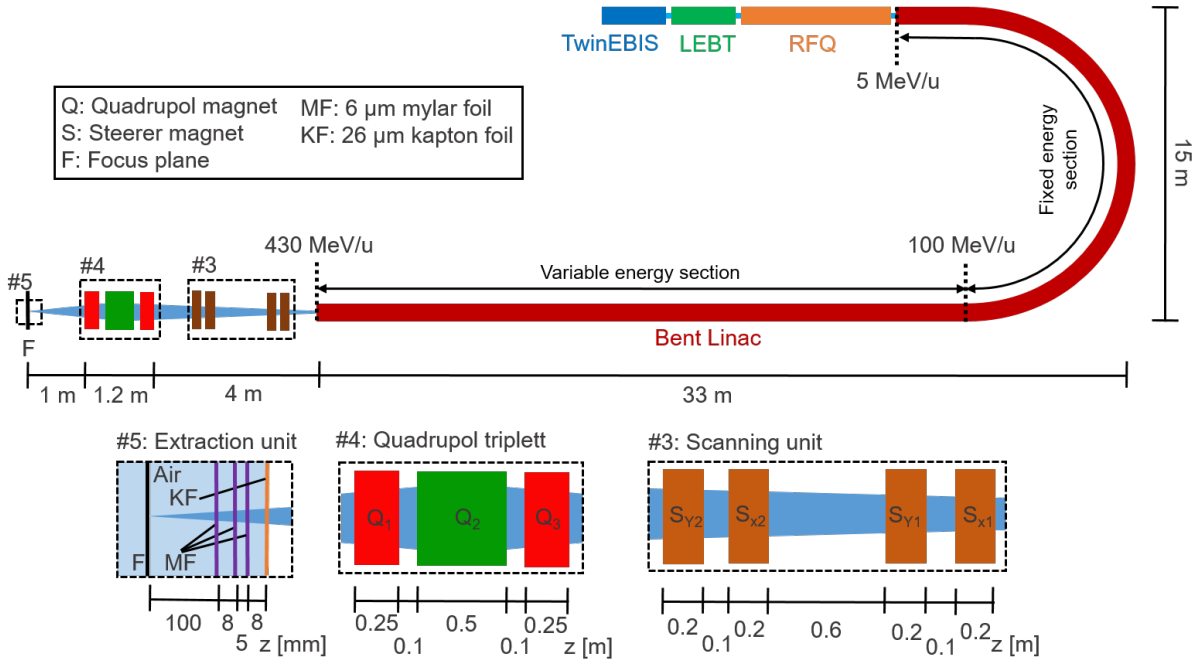

Figure 1. Concept of a carbon minibeam irradiation facility to form submillimeter $^{12}C^{6+}$ -ion beams with energies between 100 MeV/u and 430 MeV/u. Bent-LINAC concept (TwinEBIS, LEBT, RFQ and bent LINAC) is adopted from [13].

2. Hadron minibeam irradiation facility concept

Figure 1 shows the concept we suggest for a hadron minibeam irradiation facility. It is based on a bent carbon LINAC concept currently being developed at CERN and funded by the CERN Knowledge Transfer Office as part of the NIMMS project [12,13]. This LINAC concept consists of 5 substructures. A TwinEBIS source [14,15] delivers $^{12}C^{6+}$ -ions. The ions are initially accelerated and transferred to a subsequent RFQ accelerator by the Low Energy Beam Transport (LEBT). The RFQ accelerates the carbon ions to 5 MeV/u [16]. It operates at a frequency of 750 MHz, allowing a bunch-to-bunch injection into the subsequent 3 GHz bent LINAC structure which can be divided into two parts. The fixed energy section accelerates the ions to 100 MeV/u and does not allow an energy variation due to the dipole magnets in the "arc part". The subsequent variable energy section allows an energy variation of the carbon ions from 100 MeV/u to 430 MeV/u at a mean beam current of 30 nA. The advantage of a bent accelerator over a straight accelerator chain is the reduced space required for future irradiation facilities.

For (pre)clinical minibeam application, several components are added downstream of the bend-Linac which have already been designed similarly for a proton minibeam irradiation facility [17,18]: To focus the beam to a transverse width in the submillimeter range (minibeams) on the target (F in figure 1), a quadrupole triplet is used (see #4, figure 1). To scan the minibeam over the target, a scanning unit (see #3, figure 1) is placed upstream of the quadrupole triplet. It consists of two steerer magnets which first deflect the beam in X- and Y-direction (SX1 and SY1)

and two steerer magnets to bend the beam back in the opposite direction (SX2 and SY2). This arrangement allows the beam to pass the quadrupole triplet as close as possible to the optical axis, minimizing abberations. The beam extraction to air is achieved via a 25 µm thick Kapton foil. An air-filled dosimetry chamber (ionization chamber) is provided for dose monitoring. It consists of two 6 µm thick aluminium-coated Mylar foils. The side not shielded by the beam tube is covered by another aluminium-coated Mylar foil.

3. Carbon minibeam simulations

The quadruple triplet (#4 in figure 1) and the scanning unit (#3 in figure 1) are designed using the beam dynamics simulation software Trace 3-D [19] and TRAVEL [20]. Subsequently, the Geant4 toolkit TOPAS [21] was used to verify the beam dynamics and evaluate the interaction of the beam with the extraction window, the dosimetry chamber, and the air gap to the target. The 100 MeV/u and 430 MeV/u $^{12}C^{6+}$ beam of the bent LINAC serves as starting point for all simulations. Figure 2 shows exemplarily the transverse phase space of the 430 MeV/u beam at the end of the LINAC. The energy spread corresponds to 0.1% for both energies.

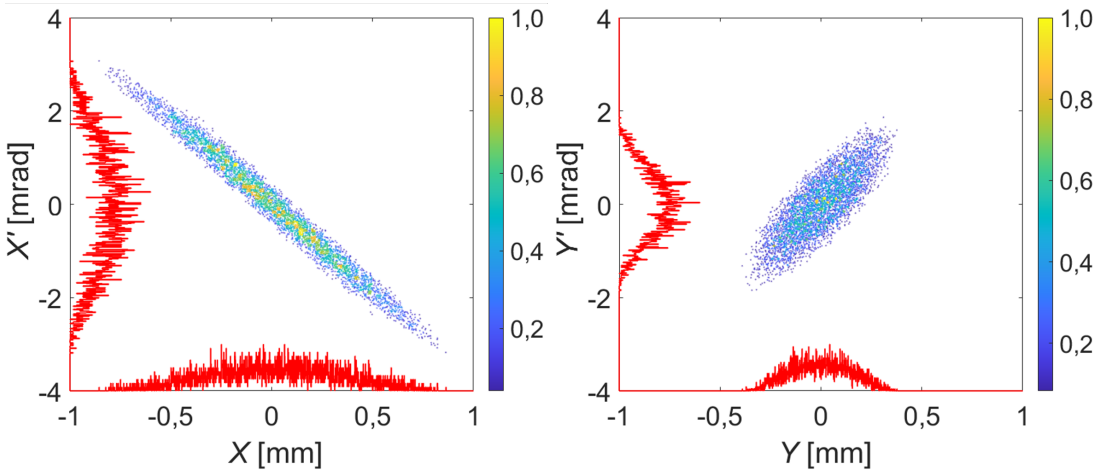

Figure 2. Transverse phase space of the 430 MeV/u bent LINAC $^{12}C^{6+}$ beam.

Figure 3 shows exemplarily the (x)-projection of the $^{12}C^{6+}$-ion distribution at the focal plane (F, figure 1) as simulated by TOPAS. Red represents the 100 MeV/u and blue the 430 MeV/u beams. The associated dashed lines represent the (x)-projection of the maximum deflected 430 MeV/u and 100 MeV/u beams at positions X = Y = +17 mm and X = Y = +38 mm, respectively. The field strengths of the qaudrupole triplet magnets Q1, Q2 and Q3 (see #4 figure 1) required to focus the beams are given in table 1. The magnetic fields of the steerer magnets S_{x1}, S_{y1}, S_{x2} and S_{y2} (see #3 figure 1) which allow the maximum deflection are given in table 2. A transverse beam width of (87 ± 1) µm and (64 ± 1) µm as well as a beam divergence of (2.8 ± 0.1) mrad and (3.1 ± 0.1) mrad results for the 100 MeV/u and the 430 MeV/u beam, respectively. Thereby, the given values represent the standard deviations of the particle distributions (σ). For maximum deflection, the beam spot width increases by less than 10%.

The sparing of normal tissue in minibeam therapy is limited by the dose applied between the individual minibeams and therefore by secondary particles created during the interaction of the beam with the matter. Figure 4 shows the (x)-projection at the target of the 430 MeV/u $^{12}C^{6+}$-ion distribution and additionally that of the secondary electrons and other secondary particles (protons, neutrons, etc.) resulting from fragmentation processes in exit window, dosimetry

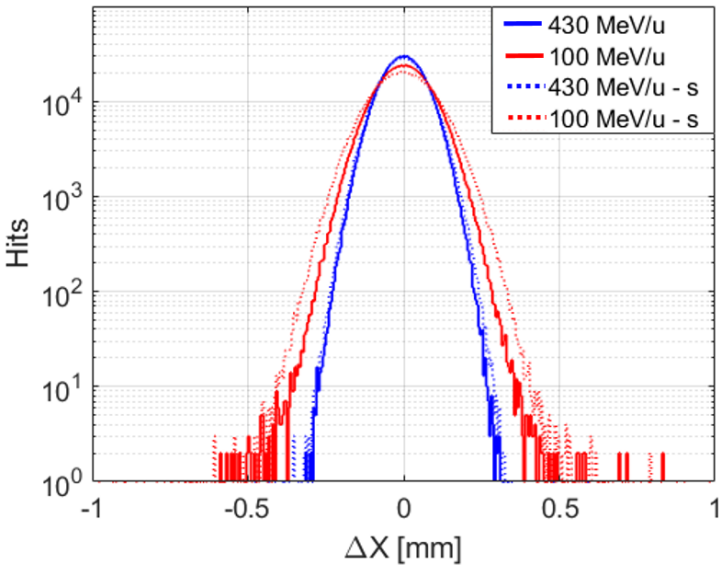

Figure 3. (x)-projection of the 100 MeV/u (red) and 430 MeV/u (blue) $^{12}C^{6+}$-ion distribution at the focal plane. The corresponding dashed lines (s) represent the maximum deflected beams on the position X = Y = +17 mm and +38 mm.

Table 1. Field strengths of the qaudrupole triplet magnets Q1, Q2 and Q3 (see #4, figure 1) for focusing the 100 MeV/u and 400 MeV/u beam.

Energy [MeV/u]	Field strengths [T/m]		
	Q_1	Q_2	Q_3
100	-18.10	15.37	-17.99
430	-40.50	34.29	-39.28

Table 2. Field strengths of the deflecting magnets S_{x1}, S_{y1}, S_{x2} and S_{y2} (see #3 figure 1) for deflecting the 430 MeV/u and 100 MeV/u beam to X = Y = +17 mm and X = Y = +38 mm, respectively.

Steerer magnet	Magnetic fields [mT]
S_{x1}	133
S_{y1}	81
S_{x2}	400
S_{y2}	350

chamber and air gap. The dose between the individual minibeams at the target entry results from the broadly distributed secondary particles of all minibeams in a minibeam array.

For clinically relevant minibeam arrays, the resulting reduction of the Peak to valley (energy) dose ratio (PV(E)DR) is evaluated with TOPAS. Therefore, the interaction of a water phantom positioned downstream to F with an array of 99 x 99 quadratic arrangement minibeams is simulated. Figure 5 shows the dose distribution at phantom entrance for the minibeam unit cell in the centre of the array exemplary for the 430 MeV/u beams. $N_{\mathrm{MB}}X$ and $N_{\mathrm{MB}}Y$ indicate the minibeam number in X and Y direction, respectively. The PV(E)DR is calculated as the ratio of

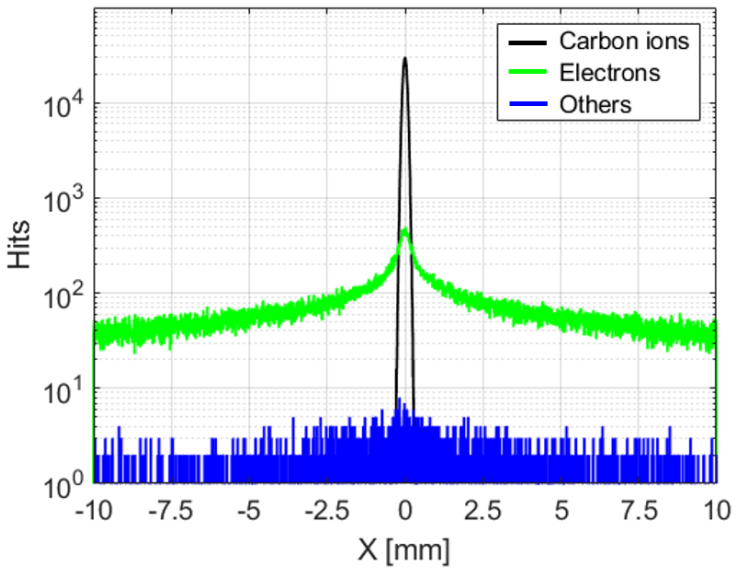

Figure 4. Transverse distribution of 430 MeV/u carbon ions and secondary particels at the focal plane.

maximum dose in the channel (green cross) and averaged dose in an area between the channels (green circle). The ctc was chosen to result in a homogeneous transverse energy dose at the Bragg peak (in water). For beam energies of 100 MeV/u and 430 MeV/u with the associated ctc's of 1.1 mm and 3.4 mm, a PV(E)DR of around 1200 and 2700 results, respectively. The array of 99 minibeams corresponds to a transverse tumor dimension > 100 mm.

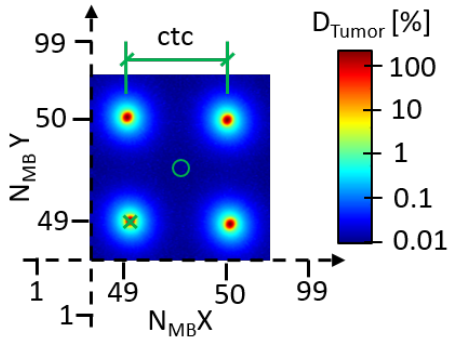

Figure 5. Unit cell of a 99 x 99 minibeam array. The green cross marks the highest and the green circle the lowest dose.

4. Conclusion

The bent carbon LINAC concepts currently under development [13] offer a high brillant beam with a constant average beam current of 30 nA for beam energies between 100 MeV/u and 430 MeV/u (approx. 3 to 30 cm range in water). Using the presented quadrupole triplet, transverse beam sizes below 100 µm (σ) at the patient are achieved although the beam scatters due to the extraction foil, dosimetry unit and air gap. The scanning unit enables a beam deflection of $> \pm 15$ mm. A PV(E)DR of > 1000 is achieved at the patient entrance. However, RBE corrected biological dose distribution in particular in the valley dose regions requires further investigations. The presented concept is a promising (and first) approach for a hadron minibeam irradiation facility. It exceeds all requirements for the planned (pre-)clinical studies defined in the introduction. Besides $^{12}C^{6+}$, theoretically, all ions with the identical mass-to-charge ratio can be accelerated by the bent-Linac. In particular, the presented system also has the potential for $^{4}He^{2+}$ minibeam therapy.

References

[1] Zlobinskaya O *et al.* 2013 *Radiat. Environ. Biophys.* **52** pp 123–33
[2] Prezado Y *et al.* 2013 *Med. Phys.* **40** 031712
[3] Datzmann G *et al.* 2020 *Front. Phys.* **8** 471
[4] Meyer J *et al.* 2018 *BJR* **92** 20180466
[5] Sammer M *et al.* 2021 *Sci. Rep.* **11** pp 1–16
[6] Girst S *et al.* 2016 *Int. J. Radiat. Oncol. Biol. Phys.* **95** pp 234–41
[7] Prezado Y *et al.* 2017 *Sci. Rep.* **7** 14403
[8] Sammer M *et al.* 2019 *PLoS One* **7** e0221454
[9] Sammer M *et al.* 2019 *PLoS One* **14** e0224873
[10] Dilmanian A *et al.* 2012 *Int. J. Radiat. Oncol. Biol. Phys.* **14** e0224873
[11] Martínez-Rovira I *et al.* 2017 *Med. Phys.* **44** pp 4223–29
[12] Vretenar M *et al.* 2021 *Proc. 12th Int. Particle Accelerator Conf. (IPAC'21)* (Campinas, Brazil) pp 1240–43
[13] Bencini V 2020 Design of a novel linear accelerator for carbon ion therapy PhD Thesis Università di Roma
[14] Breitenfeldt M *et al.* 2017 *Nucl. Instrum. Methods Phys. Res., Sect.* A **856** pp 139–46
[15] Pahl H *et al.* 2018 *J. Instrum.* **13** P08012
[16] Bencini V *et al.* 2020 *Phys. Rev. Accel. Beams* **23** 122003
[17] Mayerhofer M *et al.* 2021 *Med. Phys.* **48** pp 2733–49
[18] Mayerhofer M *et al.* 2021 *PLoS One* **16** e0258477
[19] Crandall K *et al.* 1987 Trace 3-D documentation Los Alamos National Laboratory
[20] Perrin A *et al.* 2003 Travel v4.06 user manual CERN internal note
[21] Perl J *et al.* 2012 *Med. Phys.* **39** pp 6818-37